A Study on the Seismic Dynamic Response of Deeply Buried Tunnels Crossing Faults under Different Fault Conditions

Sijie Zhou[1,*], Zelin Yan[2], Songlin Li[1], Binlin Wang[2]
[1]College of Water Resource and Hydropower, Sichuan University, Chengdu, China
[2]College of Architecture and Environment, Sichuan University, Chengdu, China
**Corresponding Author*

Abstract: Tunnels in the high-altitude, seismically active regions of Sichuan and Tibet often face hazards from both earthquakes and active faults. However, how fault geometry affects tunnel response has received limited attention. This study takes a tunnel under construction on the Qinghai-Tibet Plateau as an example. A 3D numerical model was built using FLAC^{3D} to see how the maximum principal stress in the lining changes with fault width from 20 m to 50 m and with fault dip angle from 25° to 90°. In all cases, the stress peaks at the crown and invert. These two locations are therefore the most important for seismic design. Lining stress increases as fault width increases, and decreases as fault dip increases. A dip angle of 25° gives the highest stress. In addition, the fault influence area becomes much wider when the fault is wider or when the dip angle is smaller. These results can help guide the seismic design of tunnels that cross active faults.

Keywords: Fault Zone; Seismic Response; Fault Width; Fault Dip

1. Introduction

The eastern and southern margins of the Qinghai-Tibet Plateau are experiencing intense active uplift, and a number of strategic transportation projects connecting Sichuan and Tibet are currently being built in this region. Seismic design intensities here generally reach VII or higher. With dramatic topographic relief and extremely complex geological conditions, ensuring the safety and long-term performance of tunnels that encounter complex geological defects during construction and operation represents a major scientific and engineering challenge. The study area contains more than 590 fault zones, making it nearly inevitable that deep-buried long tunnels will cross fault fracture zones. When an earthquake hits, fault zones will reflect, focus, and transmit seismic waves. That makes the tunnel shake more violently [1,2] and raises the risk of lining damage or total failure [3,4]. So in seismic design, the sections that cross fault zones are critical locations. It is important to understand how they respond to earthquake loading and to identify which parts and zones need the most attention. This matters for the seismic design of underground tunnels.

Research on the seismic response of tunnels falls into four main technical approaches: seismic damage surveys and field observations [5], physical model testing [6], numerical simulation [7], and theoretical analysis [8]. Of all these methods, numerical simulation is used the most. It gives you a lot of flexibility without costing much. Tang et al. [9] found that torsional deformation and extreme forces concentrate in the fault zone and at stiffness-mismatched interfaces. Subsequently, Kang et al. [10] adopted FLAC^{3D} to study the dynamic response of subway tunnels under strong ground motion coupled with differential settlement in ground fissure sites.

There is a lot of research on tunnel seismic response behavior. However, the most studies has been dedicated to the seismic dynamic response of intact tunnels or the evolution of dynamic response patterns in tunnels crossing faults under seismic excitation. More research is required on the way tunnels traversing faults behave under earthquake shaking.

2. Engineering Background and Model Setup

This section covers the ground conditions of the site and the essential tunnel model properties.

2.1 Geological Setting of the Tunnel Site

The tunnel site is in the high-mountain canyon region of the Qinghai-Tibet Plateau. The terrain is rough with steep slopes, deep valleys, and big elevation changes. The geology is very complex,

 Copyright @ STEMM Institute Press

and this is a high-intensity seismic zone. And the rocks are mainly schist with sandstone interbeds from the Permian Laigu Formation, plus Yanshanian diorite.

2.2 Model Setup

The model extends 150 m along the tunnel on each side of its intersection with the fault. The tunnel is circular with an external diameter of 10.2 m. The primary support is 0.15 m thick and a 0.3 m thick layer of C30 concrete forms the secondary lining. Figure 1 shows the section geometry.

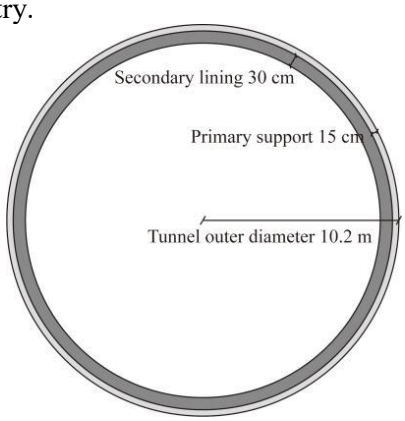

Figure 1. Schematic of the Lining Cross-Section

According to previous studies, a model extent of 6 to 8 times the tunnel diameter is enough to avoid boundary effects from excavation-induced stress redistribution. We therefore set the model width and vertical height to 70 m, the fault zone width to 40 m, and the fault dip angle to 75 °, as shown in Figure 2. We used solid elements for the primary support, which is 15 cm thick, and for the surrounding rock and fault fracture zone, both with a Mohr-Coulomb constitutive model. The secondary lining was simulated with FLAC^{3D} shell elements. Table 1 shows the material parameters.

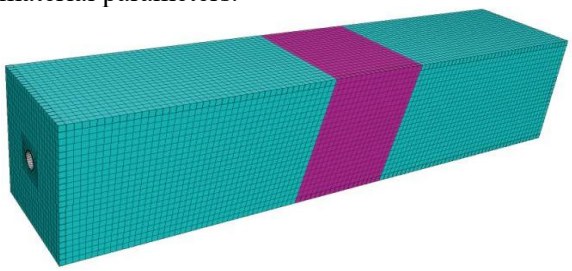

Figure 2. 3D Model of the Tunnel

Table 1. Table of Material Parameters

Model location	ρ (kg/m^3)	E (GPa)	ν	c (MPa)	φ(°)
Surrounding rock	2450	6	0.27	0.6	30
Fault fracture zone	2000	1.2	0.35	0.3	20
Primary support	2500	28	0.22	/	/
Secondary lining	2600	30	0.2	/	/

This study used the first 10 seconds of the widely known EI-Centro wave as the seismic input. As shown in Figure 3, the seismic signal was scaled to a peak acceleration of 0.15 g, followed by baseline adjustment and bandpass filtering.

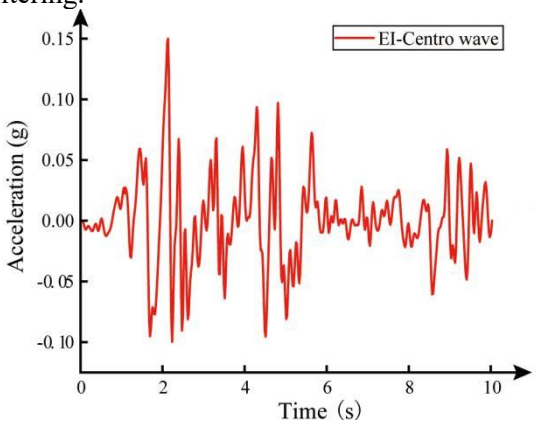

Figure 3. EI-Centro Wave

Monitoring sections were placed along the tunnel axis. The geology near the fault zone is complex. So we used non-uniform spacing. Sections are 10 m apart inside the fault zone, and 20 m apart further away where the fault influence fades. Each section has eight monitoring points: crown (C), left and right haunch (LH, RH), left and right sidewall (LSH, RSH), left and right springline (LSL, RSL), and invert (I). Figure 4 shows the layout.

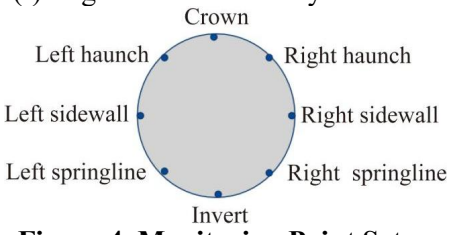

Figure 4. Monitoring Point Setup

3. Results

Stress across the fault center and along the crown for various fault widths and inclination angles. Different widths and angles give different distributions.

3.1 Analysis of Simulation Results for Different Fault Widths

Fault zone width affects three things: the overall stiffness of the tunnel-rock system, how much seismic waves reflect and overlap inside the fault, and how well the wall rocks on either side constrains the fault. So width is a key factor in the way tunnels crossing faults behave under earthquake shaking. This paper looks at how the maximum principal stress experienced by the

Copyright @ STEMM Institute Press

tunnel evolves with fault width. All other parameters are kept constant; only the fault width varies. Four widths are considered: 20 m, 30 m, 40 m, and 50 m. The goal is to see how the peak stress changes with width and to identify which locations and sections need the most attention in seismic design. Table 2 lists the results for these four widths. The data on the left and right sides are almost identical. Figure 5 also shows the results.

Table 2. Peak Maximum Principal Stress at Fault Central Section for Different Fault Widths (MPa)

Fault width (m)	C	LH	LSW	LSL	I
20	1.82	1.34	1.53	1.26	1.60
30	2.05	1.52	1.73	1.43	1.81
40	2.16	1.65	1.86	1.55	1.93
50	2.29	1.69	1.93	1.59	2.02

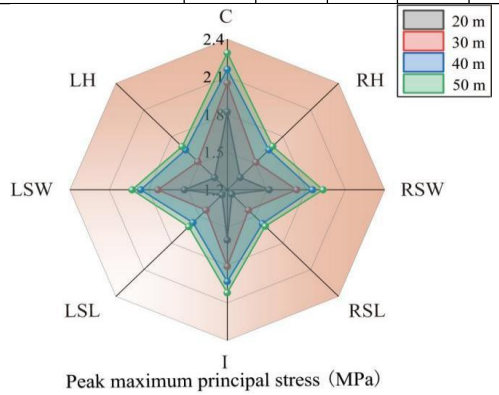

Figure 5. Distribution of Peak Values of the Maximum Principal Stress Response at the Centre of the Fault for Different Fault Widths

Table 2 and Figure 5 show that fault width does not affect where the maximum principal stress appears on the tunnel. No matter the fault width, the crown and invert always have the highest stress. So they should be the main focus of seismic design. Meanwhile, we can find that the wider the fault zone, the higher the peak stress in the lining. A wider fault means the broken rock constrains the lining less. During an earthquake, the lining can deform more freely, which creates stronger hoop tension. And the solid rock on both sides cannot hold a wide fault as tightly, so the lining inside the fault vibrates more and the stress gets even larger. For example, with the fault width increases from 20 m to 30 m, 40 m, and 50 m, the maximum principal stress at the crown rises by 12.6%, 5.4%, and 6.0% respectively. Across the whole lining section, the average increases are 12.2%, 6.3%, and 5.8%. The stress growth rate slows as the fault gets wider.

Data along the tunnel axis for different fault widths are plotted in Figure 6. And we can see all four cases show the same pattern. Stress goes up near the fault and then drops as you move away. The peak always appears at the fault center, Y = 150 m. So the peak location does not change with fault width, and the fault zone is always the most stressed region. Meanwhile, we can find that a wider fault spreads its influence farther into the surrounding rock on both sides. For a 20 m wide fault, the influence reaches Y = 180 m. For a 50 m wide fault, it reaches Y = 220 m. Every 10 m increase in fault width means the seismic design zone must be extended by 10 to 15 m on each side. This covers the extra stress from seismic energy spreading and lining vibration.

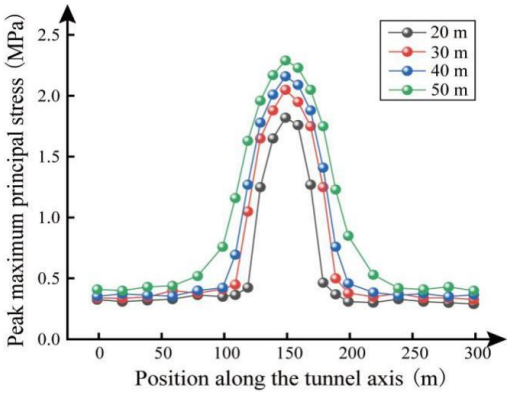

Figure 6. Distribution of the Peak Maximum Principal Stress Response at the Crown along the Axis for Different Fault Widths

3.2 Analysis of Simulation Results for Different Fault Dip Angles

Fault dip angle controls the reflection, travel, and focusing of seismic waves on the fault plane, which strongly influences the seismic response of tunnels crossing fractured fault zones. In this subsection, all other parameters are kept constant. Only the fault dip angle changes. Four dip angles are tested: 25°, 50°, 75°, and 90°. For each dip angle, the peak maximum principal stress is extracted at different points on the fault center cross-section. Table 3 lists the results. Figure 7 shows how the stress varies across the cross-section.

Table 3. Peak Maximum Principal Stress at Fault Central Section for Different Ault Dip Angles (MPa)

Dip angles	C	LH	LSW	LSL	I
25°	2.61	1.93	2.20	1.82	2.31
50°	2.32	1.71	1.94	1.63	2.05
75°	2.16	1.65	1.86	1.57	1.93

 Copyright @ STEMM Institute Press

90°	1.85	1.38	1.57	1.31	1.64

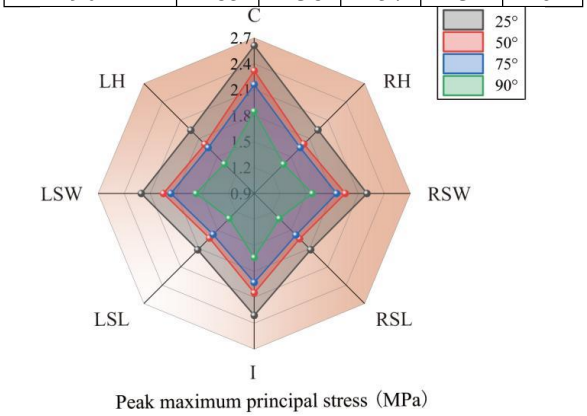

Figure 7. Distribution of Peak Values of the Maximum Principal Stress Response at the Centre of the Fault Plane for Different Fault Dip Angles

Table 3 and Figure 7 show that fault dip angle does not change where the maximum principal stress appears on the tunnel. For all four dip angles, the stress is highest at the crown and invert, lower at the sidewall, and lowest at the haunch and springline. So the crown and invert are always the key spots for seismic design, no matter the dip angle. The lining stress goes down as the dip angle goes up. The most unfavorable dip angle is 25°, which gives the highest stress. For instance, at the tunnel crown, as the dip angle drops from 90° to 25°, the stress rises from 1.85 MPa to 2.61 MPa, an increase of 41.1%. This happens for two reasons. First, when the dip angle is small, the tunnel crosses the fault over a longer length, and the hanging wall moves differently from the tunnel. Secondly, from the rock and fault parameters, we get a critical angle for wave conversion of about 30°. A dip angle of 25° is close to this critical angle, so wave conversion is strong. At high dip angles like 75° to 90°, the fault plane is almost parallel to the wave direction, so reflection and wave conversion are much weaker. That is why the stress stays low.

Similarly, when the axial data at different dip angles are plotted as depicted in Figure 8, it can be seen that all four cases show the same pattern. Stress rises near the fault and then drops as you move away. The peak always appears at the fault center. The fault influence zone gets much wider when the dip angle is smaller. For a vertical fault at 90°, the zone that needs seismic design extends 20 to 30 m on each side of the fault. For a dip angle of 50°, it must reach 30 m on each side. For a low angle of 25°, it must reach 40 to 50 m on each side.

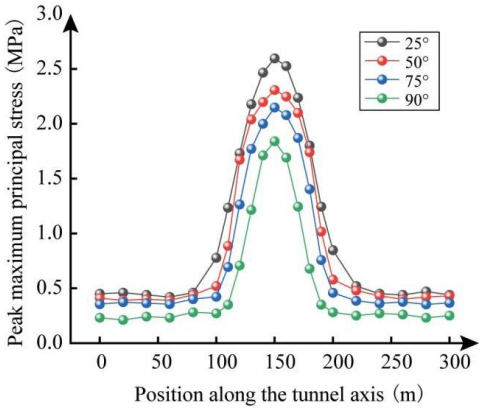

Figure 8. Distribution of the Peak Maximum Principal Stress Response at the Crown along the Axis for Different Fault Dip Angles

4. Conclusion

This study examines how fault width and fault dip angle affect the peak maximum principal stress in the lining of a tunnel crossing a fault. The main conclusions are outlined as follows:

(1) Neither fault width nor fault dip angle changes where the maximum principal stress appears on the lining section. In all cases, the stress is highest at the crown and invert, lower at the sidewall, and lowest at the haunch and springline. Therefore, the crown and invert are always the most critical locations for seismic design.

(2) The peak maximum principal stress increases with fault width. A wider fault means the broken zone constrains the lining less. The fault influence zone also expands as width increases. On average, every 10 m increase in fault width requires extending the seismic design zone by 10 to 15 m.

(3) As fault dip increases, the maximum principal stress in the rock decreases. In this study, the highest stress occurs at 25°. The stress peak stays at the fault center. At small dip angles, the fault influence zone becomes much wider.

References

[1] Song S, Shen Y, Yu Y, et al. Shaking table test on seismic response and failure characteristics of buried pipeline-tunnel structure crossing fault fracture zone. Tunnelling and Underground Space Technology incorporating Trenchless Technology Research, 2026, 167: 107006.

[2] Tang J, He M, Qiao Y, et al. Analytical solution for longitudinal responses of tunnels under combined effects of seismic

waves and strike-slip faulting. Journal of Rock Mechanics and Geotechnical Engineering, 2026, 18(2): 1266-1289.

[3] Asakura T, Sato Y. Mountain tunnels damage in the 1995 Hyogoken-nanbu Earthquake. Quarterly Report-RTRI, 1998, 39: 9-16.

[4] Wang T-T, Kwok O-LA, Jeng F-S. Seismic response of tunnels revealed in two decades following the 1999 Chi-Chi earthquake (Mw 7.6) in Taiwan: A review. Engineering Geology, 2021, 287: 106090.

[5] Sharma S, Judd WR. Underground opening damage from earthquakes. Engineering Geology, 1991, 30(3-4): 263-276.

[6] Lv Z, Li J, Jin J. Seismic Responses in Shaking Table Tests of Spatial Crossing Tunnels. Buildings, 2026, 16(2): 312-312.

[7] Nguyen KT, Tran MN. Seismic responses of soil–twin tunnels system subjected to Rayleigh wave propagation. Soil Dynamics and Earthquake Engineering. 2026, 208: 110316-110316.

[8] Yu H, Li X, Li P. Analytical solution for vibrations of a curved tunnel on viscoelastic foundation excited by arbitrary dynamic loads. Tunnelling Underground Space Technology, 2022, 120: 104307.

[9] Tang J, He M, Qiao Y, et al. Analytical solution for longitudinal responses of tunnels under combined effects of seismic waves and strike-slip faulting. Journal of Rock Mechanics Geotechnical Engineering, 2025.

[10] Kang X, Jiang L, Bai Y, et al. Seismic damage evaluation of high-speed railway bridge components under different intensities of earthquake excitations. Engineering Structures, 2017, 152: 116-128.

 Copyright @ STEMM Institute Press